The benefits of interferometry for the characterization of extrasolar planetary systems

J. Schneider [1]

[1]Observatoire de Paris - 92195 Meudon, France

Abstract: Interferometry is a useful tool to separate planets from their parent star. In addition to make a direct detection (by a snapshot image or by visibility measurements), it can be used to provide an indirect characterization the planetary systems (their architecture, star-planet interaction etc) in different ways such as astrometry and stellar surface imaging. A comprehensive prospective review of all these approaches is given.

1   Introduction

The detection of the first planetary systems by radial velocity has provided essentially dynamic characeristics of planets, namely their orbital elements and their mass (generally up to a factor $\sin i$, i being the orbit inclination). The detection of a few planetary transits has allowed, in a limited number of cases, first steps in the physical characterization of planets, namely their radius and, in the case of HD 209458 b, the composition and dynamical behaviour of its atmosphere. It is now time to go further and deeper in the physical characterization of planets. Moreover, the radial velocity and transit methods have a decreasing sensitivity, in terms of probability of detection and of minimum planet mass, with increasing orbital distance. On the contrary, astrometry and imaging are more efficient for moderate or large planet-to-star distances.

There are two main goals for the planetary system characterization:

1. Census of planetary systems in the Galaxy and their characteristics. This goal calls for the detection of as many planets as possible.

2. Search for life (in a limited sample of planets), leading to a special attention of Earth-like planets in the "Habitable Zone" (HZ) of their parent star (where the temperature allows for liquid water).

While the first goal is of great importance from a general astrophysical point of view, the second goal is part of profound inquiries on the presence and forms of life elsewhere in the Universe.

I will not discuss here instrumental aspects such as the problem of finding bright reference stars for faint objects or atmospheric turbulence.

2   What we want to learn about extrasolar planets

Table 1 presents on the left side the major characteristics of extrasolar planets which we can hope to measure in a reasonable future. The right side of the table summarizes the methods by which we can access these characteristics. The art is then to cross-correlate the questions on planet characteristics with the means of planet detection. The only presently successful detection methods, radial velocity and transits have up to now (December 2004) provided more than 150 planets. An updated catalog of planets can be found at www.obspm.fr/planets.

<div align="center">

Table 1 - Planet observables /vs detection methods

</div>

Planet characteristics		Detection methods
Orbit:		Star's wobble:
- P, a, e, i		- *Rad. velocity*
Mass M_{pl}		- *Astrometry*
Radius R_{pl}		- *Timing*
Temperature T_{pl}		
Albedo $A_{pl}(\lambda)$		Transits
Atmospheres and Clouds		
Environment:	$\Longleftrightarrow$	
- *Magnetospheres*		Lensing
- *Rings*		
- *Moons and binarity*		Imaging
Surf. structures:		
- *Continents*		
- *Oceans*		Radio detect.
Variations:		
- *Day, seasons*		
Life?		

3   What interferometry can do for extrasolar planets

Several methods are used or planned for the detection and characterization of exoplanets: radial velocity, timing, astrometry, microlensing, transits and imaging. Additional information comes from spectroscopy and polarimetry. Interferometry means (very) high angular resolution. It is most often associated with astrometry and imaging of the resolved star - planet system. But, as will be illustrated by several examples below, microlensing and stellar surface imaging can equally benefit from this technique.

The source morphology, resulting from the different science topics discussed below, is finally limited to a small number of configurations:

- a single circular object for astrometry;
- two ponctual objects for the resolved star - planet system, or the background - foreground star for microlensing;
- a disk surrounded by an ellipse for planets with resolvable rings;
- a large circular dark spot on the stellar disk for transiting planets;
- a circular bright spot on the stellar disk for spots generated by the star - planet interaction.

They are shown on Figure 1. The simplicity of these configurations makes the analysis of visibility measurements and image reconstruction easier.

Figure 1: The four morphologies for the characterization of planets: planet-star system (upper left); planet with a ring (upper right); transiting planet (lower left); stellar brigh spot (lower right)

.

4 Science rationale: From primary observables to planet properties.

The task of exoplanetology is to extract, in a two step process, the planet characteristics from primary observables. The primary observables are visibility function or a reconstructed image at different wavelengths (and possibly in different polarization modes). From them, one then can construct a few star and planet observables: star or planet position and flux (eventually 2D) as a function of time and wavelength. From these planet observables, a series of properties (listed in table 1) can be derived. The essential role of physical modelisation must be stressed here.

5 Detailed science cases

5.1 The two regimes of direct imaging

Let us first assume that planets are spherical. We will see below that it may not always be the case. For the exobiological purposes which is the main long term goal of the exoplanetology enterprise, we consider essentially old (and therefore cooled) planetary systems, those for which, in a conservative view, a biological activity has time to develop. The intrinsic thermal emission of the planets can thus be neglected and there are only two flux regimes for the planet illuminated by the star: reflected stellar light and thermal emission of the planet heated by the star.

5.1.1 Thermal emission

The planet heated by the star, located at a distance a from the planet, acquires an equilibrium temperature given, in absence of greenhouse effects, rotation locking etc, by

$$T_{pl} = T_* \times \left(\frac{R_*}{2a}\right)^{1/2} (1 - A_{pl})^{1/4} \tag{1}$$

where A_{pl} (generally wavelength dependent) is the planet albedo. The total planet to star flux ratio is then given by

$$\frac{F_{th}}{F_*} = \left(\frac{R_{pl}}{2a}\right)^2 \tag{2}$$

But, whereas the star's spectrum peaks at $(\lambda_*)_{max}$, the planet thermal spectrum peaks at $(\lambda_{pl})_{max} = (\lambda_*)_{max}(T_*/T_{pl})$. At $\lambda = (\lambda_{pl})_{max}$ the planet to star thermal flux ratio is typically

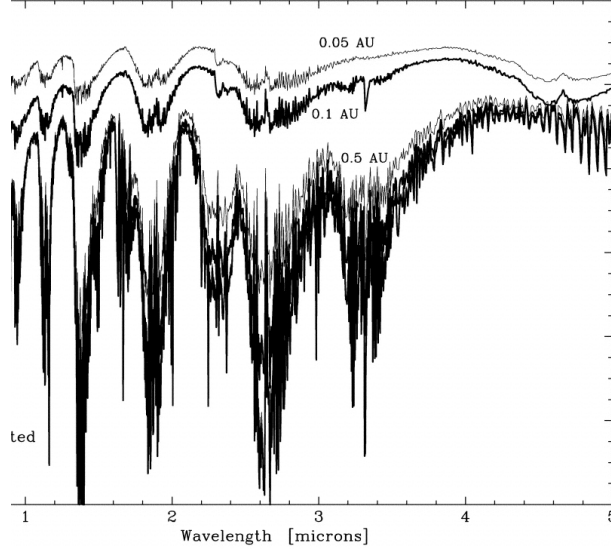$$\frac{F_{th}}{F_*} \approx 10^{-6} - 10^{-7} \tag{3}$$

Figure 2: Spectrum of a Jupiter at different distance from its parent star (Sudarsky et al 2003)

The adjustment of the planet thermal spectrum to a Planckian distribution gives T_{pl} and the flux ratio gives R_{pl}^2.

From the ground it is likely that the terrestrial atmosphere thermal background dominates the planet signal at 10μ, even in Antarctica.

5.1.2 Reflected light

In the reflected light regime, the planet to star flux ratio is given by

$$\frac{F_{refl}(t)}{F_*} = \frac{A_{pl}}{4} \times \left(\frac{R_{pl}}{a}\right)^2 \times \phi(t) \qquad (4)$$

where $\phi = \phi(P, i, e, t)$ is an orbital Keplerian phase factor. The latter helps to identify the detected object as a planet and constrains the orbital parameters. Note that this advantage is not present in the thermal emission regime.

Typically:

$$\frac{F_{refl}}{F_*} \approx 10^{-9} - 10^{-10} \qquad (5)$$

The star and the planet spectra have, roughly, the same Planckian shape. The flux ratio (4) gives access to the product $A_{pl} \times R_{pl}^2$ and the combination of F_{refl} and F_{th} gives A_{pl} and R_{pl}.

5.2 Atmospheres

The physical characterization of atmospheres is essentially made by broad band photometry or by spectroscopy. From spectrocopy we can learn what chemical species are present in the planet atmosphere and from broad band photometry we can have some hints on the atmosphere density (through the amount of Rayleigh scattering at low wavelength). For instance, Fig. 2 shows the spectrum of a Jupiter-like planet at different distances from its parent star (Sudarsky et al. 2003). For hot Jupiters (at 0.05 AU), the thermal emission at $\geq 1.5\mu$ dominates the reflected light.

For planets with a quasi-transparent atmosphere (like the Earth in the visible), there is an increase of the planet albedo toward shorter wavelength due to Rayleigh scattering. The amount of Rayleigh scattering gives an indication on the atmosphere density (above the surface of optical depth = 1; see Fig 3 (Selsis 2003).
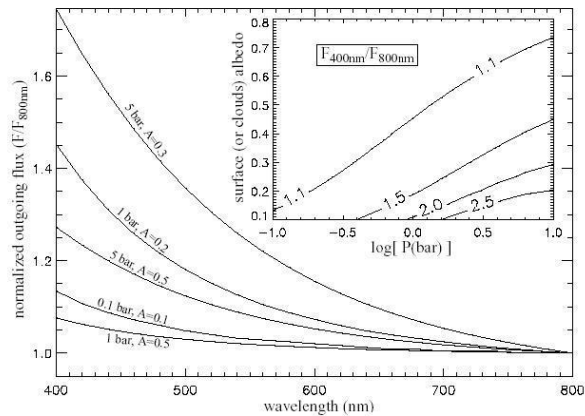
Figure 3: Rayleigh scattering spectrum for different albedos (Selsis 2003)

5.3 Benefits from variability

Even with no spectral resolution or color information, the investigation of the variability of the planet albedo provides rich information on its properties. There are two types of variations: intrinsic changes on the planet and apparent modulation induced by the planet rotation.

1. *Instrinsic variations: clouds, seasons and volcanoes*

   For an Earth-like planet, the presence or absence of a cloud coverage can change its global albedo by a factor up to 60% or more. Indeed, water vapor clouds have an albedo of 90% whereas in absence of clouds the observer sees directly the planet surface which has an albedo depending on the nature of the surface: 100% for snow, 40% for a rocky soil, 6% for oceans. A variation $\Delta S_{cl}/S_{cl}$ in the area of the cloud coverage percentage (due to climate and weather changes) leads to a variation $0.4\Delta S_{cl}/S_{cl}$ ($= 0.2$ for $\Delta S_{cl}/S_{cl} = 0.5$) in the global planet reflected flux for a rocky soil. The chaotic nature of weather changes makes this change in the planet albedo random, with a time scale depending, among other factors, on the wind speed.

   On the other hand, long term variations can be due to seasonal effects (see Fig 4 for Neptune).

   Finally, for rocky bodies, an intense volcanic activity can be present leading to an increase of the planet intrinsic flux; This is the case for Io whose flux at 5μ increases by a factor 3 during volanic activity (Fig 5).

2. *Planet rotation and surface morphology*

   Even when the planet characteristics are stationnary, their appearance can be modulated by the planet rotation combined with surface inhomogeneities (Labeyrie et al. 1999, Ford et al 2002). The period of the resulting light curve gives the planet's duration of the day. Its shape is related to the size and nature of inhomogeneities: for instance the difference $\approx 30\%$ in the albedo of oceans and rocky soils leads to a modulation of the planet brightness up to 30 %, depending of the size of inhomogeneities.

5.4 Surroundings

In the Solar System, the majority of planets are accompanied by surroundings of several kinds: rings, satellites, magnetospheres. The latter can be detected directly only by their decametric emission (Zarka 2001, Stevens 2004), although some of their indirect effects can be detected (for close-in Jupiters) in the visible through their influence on the stellar surface (see section 5.6.1).
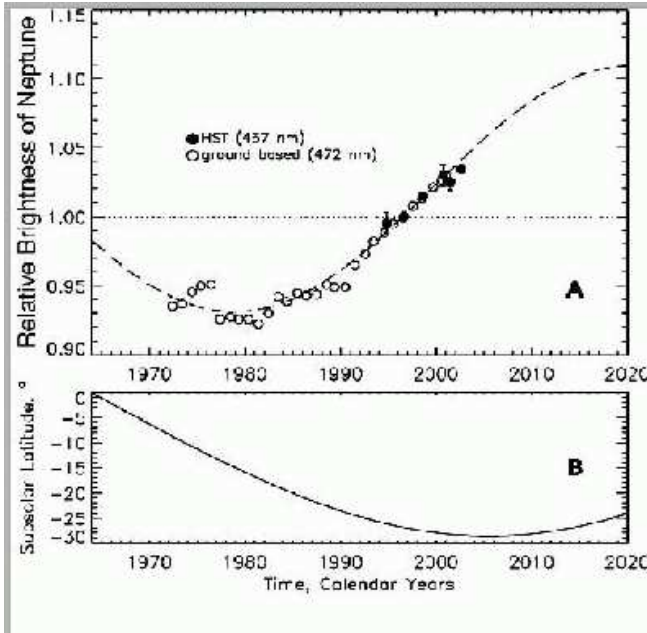
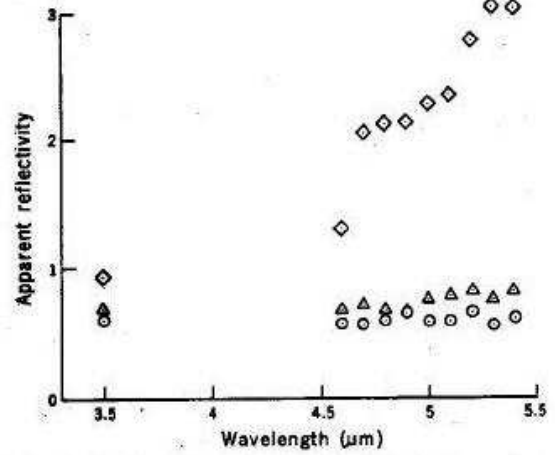Figure 4: Seasonal variation of Neptune brightness (Sromovsky et al 2003)

Figure 5: Global Io spectrum during volanic activity (diamonds) compared to quiescent phases (triangles and squares) (Witteborn et al 1979)

1. *Rings*

   The detection of rings would not only contribute to the exoplanetary zoology. It would provide some constraints on the planet mass since they are confined in the Roche limit given by $R_{Roche} = (M_{pl}/\rho)^{1/3}$, ρ being the ring material density (≈ 2). Their large size (generally twice the planet size) makes them easier to detect by imaging than the planet itself. Their presence has an important impact on the estimate of the planet radius R_{pl}. Indeed, the determination of R_{pl} is generally expected from the total amount of the thermal flux through the relation

$$F_{th} = 4\pi\sigma R_{pl}^2 \qquad (6)$$

   But this relation holds only for spherical bodies. If rings are present, the value of R_{pl} deduced from eqnuation (6) will be overestimated up to a factor 2. To check the presence of a ring and to disentangle the contribution of the ring and of the planet itself from the total flux, one can make use of the variation of the reflected flux F_{refl} along the planet orbital revolution. Indeed, during half of the orbital period, the observer sees the non-illuminated back side of rings; the latter may in addition hide a significant part of the planet, resulting in a significantly perturbed light curve (with respect to a light curve of a reflecting sphere; see Arnold & Schneider 2004).

   In addition to detect rings through the ring + planet reflected light curve, one can in principle extract them from the source morphology, either in a reconstructed image or in the planet visibility function. The ring orientation being thus determined, it gives the orientation of the planet roration axis since rings must lie in the planet equatorial plane. The planet axis in turn gives precious indications on the planet-planet interaction. The required base line is then $B = \lambda D/R_{ring}, = 1.5$ km at $\lambda = 1\mu$ for a $R_{ring} = 3R_{Jup}$ ring at 10 pc.

2. *Satellites (and binary planets ?)*

   Satellites of giant planets in the habitable zone can as well be potential sites for extrasolar life. In addition, one should be prepared to the detection of binary planets; indeed the example of the Solar System shows that binary objects with a similar size, such as binary asteroids (Merline et al 2002) and binary trans-neptunian objects (Noll 2003), are not an exception. Here again, like in the case of rings, the binary nature of the planet would change the determination of their
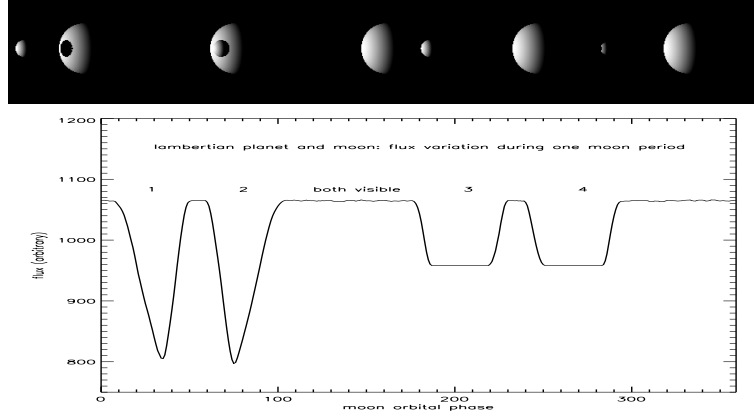
Figure 6: Light curve of the planet-satellite (or binary planet) system produces by mutual transits and shadows (Schneider et al 2003)

radius from the total flux (by a factor $(R_{pl1} + R_{pl2})/R_{pl} = $ up to $\sqrt{2}$). It would also change the mass of the planetary bodies up to a factor 2 and therefore the mass distribution of planets. In addition, the combination of the satellite orbital period, associated with the satellite-planet separation, would provide, after only 1 satellite revolution, constraints on the planet mass, even for masses unreachable to radial velocity and astrometric measurements.

There are two methods to detect a satellite or a binary planet:

- Even without resolving the satellite (or component of a binary planet) from its parent planet, one can make use of the mutual planet/satellite shadows and transits during the satellite revolution around the planet. They affect the planet + satellite light curve as shown Figure 6 (Schneider et al. 2003).

- By direct imaging: in order to resolve a binary planet with a separation S, the required baseline is $B = \lambda(D/S) = 400$ m at $\lambda = 1\mu$ and $D = 10$ pc for a typical Jupiter-Europa separation.

5.5 Parent star astrometry

The displacement of the measured position of a star with a planetary companion can due due to the actual change of its position in the star + planet barycentric system or to the displacement of the star + planet photocenter due to the planet contribution to the detected flux.

5.5.1 Dynamical wobble

The amplitude $\delta\theta_* = (M_{pl}/M_*) \times (a_{pl}/D)$ of the dynamical wobble requires a baseline $B = \lambda(M_*/M_{pl}) \times (D/a_{pl}) = 10$ km at $\lambda = 1\mu$ for a 10 Earth-mass planet at 1 AU from a star at 5 pc.

5.5.2 Photocenter wobble

Its amplitude (peak to peak) is given, in angular terms, by

$$\delta\theta_* = 2(a_{pl}/D) \times (F_{pl}/F_*) \tag{7}$$

From equation (4), the ratio F_{pl}/F_* is proportional to $(R_{pl}/a)^2$ for the reflected light. The amplitude $\delta\theta_*$ then becomes:

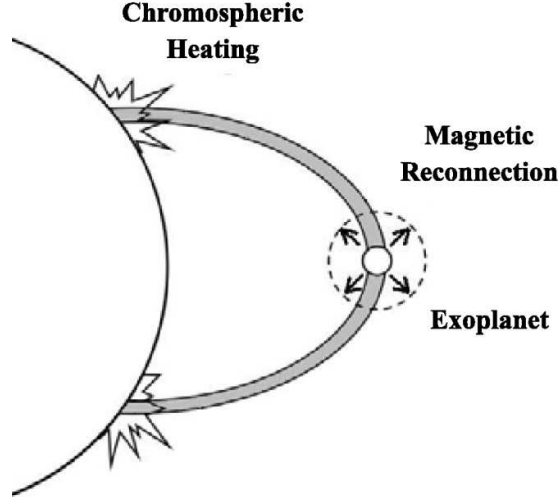$$\delta\theta_* = 2A_{pl}R_{pl}^2/(Da_{pl}) \tag{8}$$

63

Figure 7: Hot spot on a stellar surface induced by a close-in magnetic planet (Ip et al 2004)
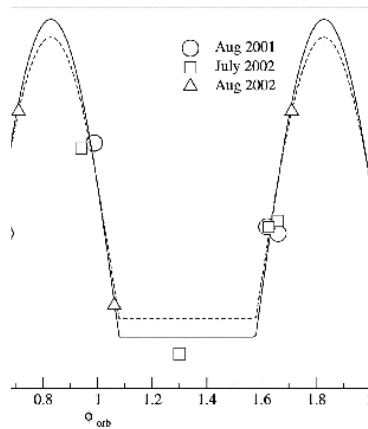

Figure 8: Ca II emission induced correlated in phase with the orbital revolution of the planet HD 179949 (Shkolnik et al 2003)

The amplitude of the photocenter wobble is thus the highest for the most close-in planets. For $a_{pl} = 0.05AU$, $R_{pl} = 1.3R_J$ and $D = 5$ pc, $\delta\theta_* = 0.15\mu$ as. Such a small wobble is unreachable from the ground.

5.6   Parent star surface imaging

Like in the case of the stellar dynamical wobble, it is possible to get some characteristics of the planet from observation of the star itself, namely of its surface imaging.

5.6.1   Planet-star interaction

Magnetized planets sufficiently close to their parent star can induce hot spots on the stellar surface (Saar et al, 2004, Ip et al 2004; see Fig 7). Whereas spots due to intrinsic stellar activity are corotating with the stellar surface, these spots remain in phase with the planet orbital revolution. They can for instance be the site of emission of spectral lines such as CaII lines. This phenomenon has been observed for HD179949 (Shkolnik et al 2003; see Fig. 8), for which

the flux variation in the CaII line is 5% integrated over the whole stellar (visible) surface. The $N \times N$ pixel imaging of the stellar surface would havee a double benefit: the signal would be increased,

in the pixel where the spot is located, by a factor N^2 and one could locate the spot on the stellar surface and compare this location with the planet orbital phase.

The required baseline is $B = \lambda ND/R_* = 400$ m at $\lambda = 0.5\mu$ for $N = 3$ resolution elements.

5.6.2 Imaging of transits

The imaging of transits improves the possibility to make a spectroscopic investigation of the planet atmosphere during the transit and provides a determination of the orbit position angle for planets very close to their star. It can then be interesting to compare this position angle with the orientation of possible outer planet orbits. For an $N \times N$ pixel imaging of the stellar surface, the planet atmosphere blocks a fraction $N^2 h R_{pl}/R_*^2$ of the stellar light, where h is the scale height of the atmosphere. (Schneider 1999). For $N = 5$ and $h = 10,000$ km this fraction is 510^{-2}

For the stellar surface imaging the required baseline is $B = \lambda ND/R_* = 700$m at $\lambda = 0.5\mu$ for $N = 5$ resolution elements.

5.7 Astrometry and imaging of microlensing events

Several microlensing events are detected each year. For some of them, a precise photometric monitoring leads to planetary candidates. The lensing light curve provides only a constraint on the projection on the sky plane of the star-planet separation at the time of observation and on the planet mass. It would be useful to have a high resolution imaging of the system in order to separate the (lensed) background star from the (lensing) foreground star in order to clarify the geometry of the configuration. For lensing events in the Galactic Bulge, the required baseline is $B = \lambda D/(3UA) = 270$ m at 1μ.

In addition, a follow up of the apparent trajectory of the lensed background star would give precious constraints on the star and planet mass (Han & Chang 2003, Gosh et 2004; see Fig 1). The apparent displacement $\delta\theta_B(t)$ of a background star located at a distance D by a foreground star having a mass M_L located at $D/2$ is

$$\delta\theta_B(t) = \frac{2GM_L}{b(t)c^2} + O\left[\left(\frac{GM_L}{bc^2}\right)^2\right] \tag{9}$$

where $b(t)$ is the "impact parameter" of the background star line of sight with respect to the foreground lens; it is a function of time due to the relative proper motion of the two stars. For $M_L = 1M_\odot$ and $b = 3AU$ $\delta\theta_B = 0.07$ mas and the corresponding required baseline is $B = 150$ m at 1μ. A more difficult objective would be to detect the deviation of the apparent trajectory of the background star by the planet itself. For a background star passing at 3 AU from the lense line of sight but at 0.1 AU of a Jupiter-mass planet orbiting the lens (no caustic configuration is needed), the required baseline would be $B = 15$ km at 1μ.

5.8 Free floatting planets

A new class of planets has recently emerged, "free-floatting" planets, i.e. planets who do not orbit around a parent star (Zapatero et al 2003, Martin 2004). One of the instrumental advantages of this situation is that it does not require a high contrast dynamics or a starlight suppression mechanism. As single ponctual objects, free floatting planets *a priori* not require high angular resolution capabilities. There are nevertheless circumstances where high angular resolution will be essential.

Let us consider different cases in increasing order of angular resolution requirements.

5.8.1 Binarity

Free floatting planets may be the result of gravitational ejection from a planetary system or of the in situ collapse of a gas + dust cloud (like in the case of brown dwarfs). In the latter case, there is probably no reason that these planets are not, sometimes, binary: the example of binary brown
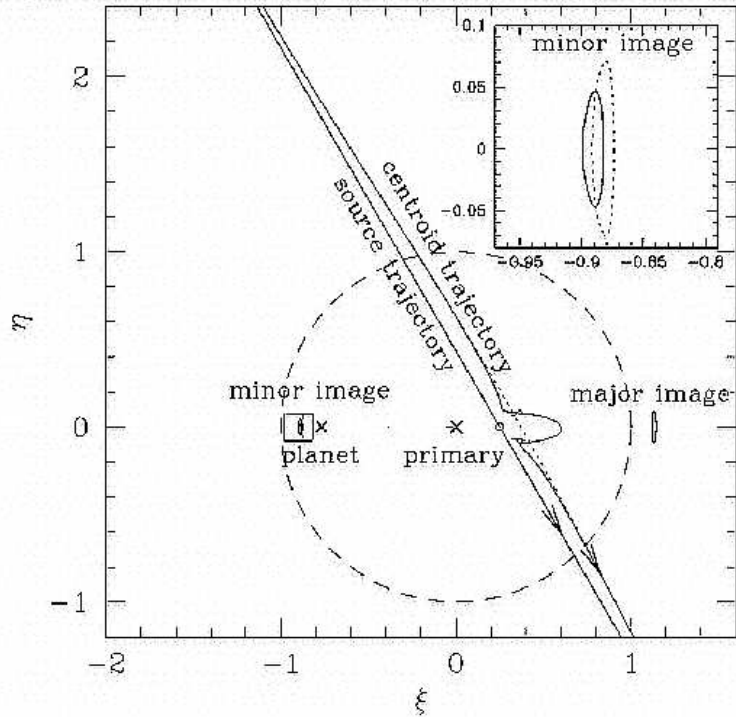
Figure 9: Gravitational displacement of a background star by a foreground star + planet system (After Han & Chang 2003)

dwarfs and of a recently discovered planet + brown dwarf system (2MASS 1207; separation 0.78 arcsec, Chauvin et al 2004) supports this hypothesis.

A separation of 0.1 AU would give a revolution period of 3 months for a binary with two 5 Jupiter mass components, opening the possibility of a dynamical determination of component masses. For a system located (like 2M1207) in a young cluster at 50-70 pc, the required baseline would be $B = 100$ m at $\lambda = 1\mu$.

5.8.2   Rings

Several disks have been observed around brown dwarfs (Liu et al. 2003). It is thus legitimate to extrapolate this observation and to speculate than rings can exist around free floatting planets. Assuming a ring three times larger than Jupiter and an inclination $i = 45^o$, a detection of its apparent ellipticity would require, for a distance of 10 pc, a baseline $B = 3$ km at 1μ.

5.8.3   Diameter

To constraint models of free floatting planets, it is important to know their radii and to compare them with the radius deduced from the emission spectrum. For a Jupiter sized planet at 10 pc, the required baseline would be $B = 6$ km at 1μ.

5.8.4   Surface inhomogeneities ("red spot")

Periodic variability in brown dwarf brighness reveals the existence of surface inhomogeneities. They can as well be present on free floatting planet surface. No high angular resolution is required at this point. But the direct imaging of these inhomogeneities would help to clarify their morphology.

The required baseline for an 3×3 pixel image for a free floatting Jupiter at 10 pc is $B = 18$ km.
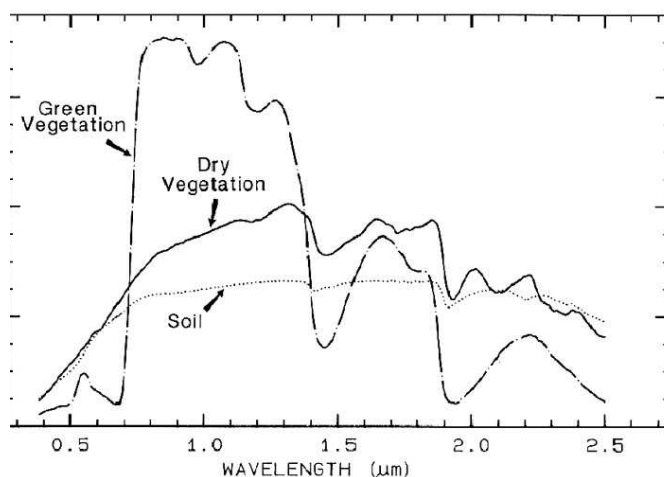
Figure 10: "Vegetation Red Edge" at 725 nm measured for two types of vegetation (Clarck 1999).

5.9 Biosignatures

In the stard view, only Earth-like planets can support life. For such planets, a biosignature is an observable believed to be indicative of a biological activity. There are two types of spectral biosignatures: surface and atmospheric. Atmospheric signatures are absorption bands characteristic of species believed to be rejected in the atmosphere by any kind of biological activity. The nature of the latter remains an open question, but very far from equilibrium abundance of species is considered as a sufficient criterion of bio-activity. The most promising atmospheric spectral biosignature is the combination of water, oxygen, ozone and carbon dioxyde, although an abiotic origin of oxygen and ozone has not yet been completely investigated.

Surface biosignatures are spectral features of the planet surface characteristic of an analog of terrestrial vegetation. This kind of feature has gained some interest after the recognition that for all kind of terrestrial vegetation there is a common "vegetation red edge", i.e. an important and sharp increase in the reflectance of vegetation at 725 nm (see Fig 12). Moreover, an observational test has shown that this VRE would be detectable in the global spectrum of an analog of the Earth located at 10 pc (Arnold et al 2002; see Fig 11).

An essential requirement is the wavelength range and resolution. From the ground it would be very difficult to disentangle the contribution of the Earth atmosphere (water, oxygen, carbon dioxyde) from most of the possible atmospheric signatures of biological interest on an exo-Earth. Only a large amount of methane could be detected. The only tractable biosignature would be an analog of the vegetation colours. Such an analog would consist of a spectral feature such as the terrestrial vegetation red-edge at 725 nm but probably at different (and unpredictible) wavelengths. This kind of feature could be identified as a possible biosignature by its absence in mineral reflectance spectra. Note that minerals with sharp edges in their spectra are rare species (such as cinnabar) and not wide spread like vegetation. That is why the vegetation red edge is visible on a global Earth spectrum represented in Figure 11.

6 Summary of requirements

Contrary to the majority of other scientific objectives of interferometry, the separation of an extrasolar planet from its parent star requires an extremely high dynamical range. This requirement has nevertheless no impact on the global architecture of an interferometer (in terms of baseline, number and diameter of sub-apertures). But it has an impact on the focal instrumentation at the recombiner
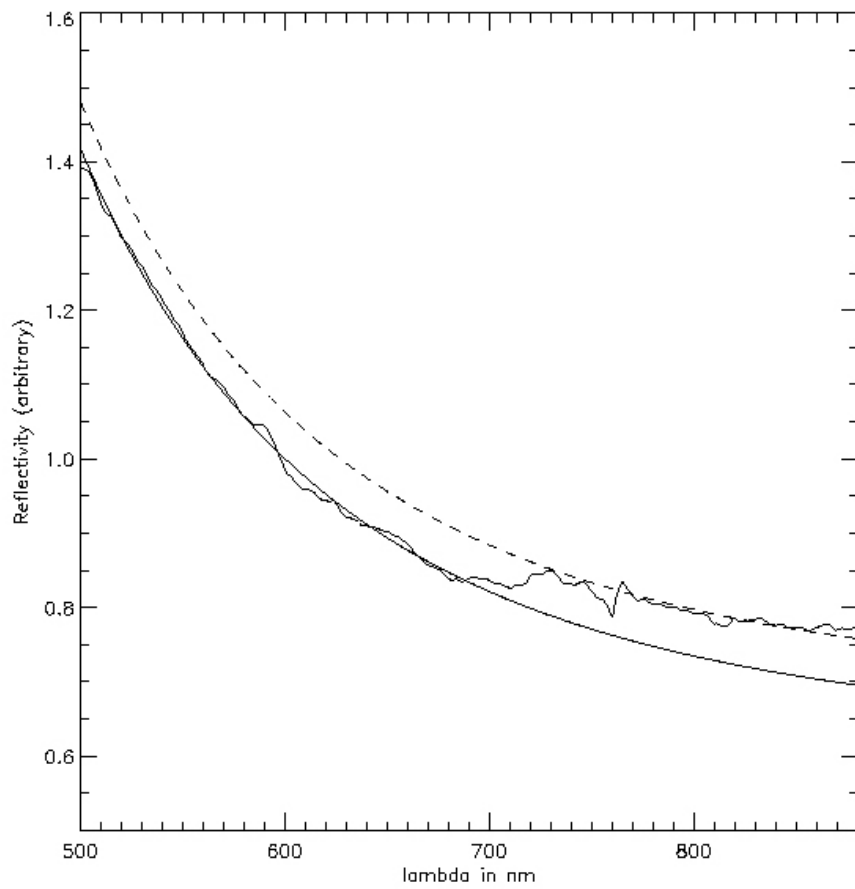
Figure 11: "Vegetation Red Edge" at 725 nm detected in the Earthshine (Anold et al 2002). The increase in the spectrum toward lower wavelength corresponds to the Rayleigh scattering by the Earth atmosphere.

(star light suppression mechanism) and the quality of the adaptive optics for each sub-aperture.

The science objectives briefly presented above lead to constraints on the different observables, namely angular resolution (for imaging), limiting magntitude (for the faintest objects), magnitude accuracy (for brightness variations), spectral resolution (for atmosphere spectra) and maximum exposure time (for transient phenomena).

An Earth in the HZ of a G star with $m = 5$ has a magnitude $m = 30$ and gives, in the 400-1000 nm total range N = 120ϵA photons/hour, where ϵ is the end to end efficiency and A the collecting area in square meters. For ϵ =1% and A = 500 m^2, N = 700 photon/hour. Assuming that the photon noise dominates speckle noise and detector noise, for an SNR = 7, the detection times for different features (Rayleigh scattering with R = 3, CH4, vegetation red edge) range from 0.5 to 20 hours. To detect albedo variations of 30% for an Earth with an SNR = 5, the required exposure time is 100 h. The exposure can be fragmented into elementary short exposures (for instance 30 min) in which the planet is not detected individually. We infer that a photometric precision of 6% or better is required.

The quantitative estimates of the other requirements are summarized in Table 2.

Table 2 - Summary of the science requirements

Science objective	Science requirements				
	Ang. Res.	Mag. lim.	Mag. Accur.	Spectr. Res.	T. Res.
Terr. planet detection		30			
Giant pl. atmosph.		25		100	
Rayleigh scatt. ($\oplus$)		30		5	
Brightness variations		30	6%		1 h.
Ring imag.	0.15 mas	20-25			
Pl. binarity	0.5 mas				
Astrometry (10 $M_\oplus$ at 1 AU)	20 μas	10			
Star surf. imaging	0.15 mas				
Planet mass by microlens.	50 μas				
Giant planet radius	35 μas	25			
Giant planet $N \times N$ cartogr.	10 μas	25			
Biosign.		30		10	

These requirements translate into two main characteristics of the intrument architecture, namely baseline (from the angular resolution) and collecting area resulting from the total number of recorded photons required for the other parameters (limiting magnitude, magnitude accuracy, spectral and temporal resolution).

<div align="center">**Table 3 - Instrumental requirements**</div>

Science objectives	Baseline	Collecting area (m^2)
Terrestrial planet detection		200
Giant planet atmospheres		200
Rayleigh scattering ($\oplus$)		1000
Brightness variations (giant pl.)		200
Ring imag.	1.5 km	
Planet binarity	400 m	
Astrometry (10 $M_\oplus$ at 1 AU)	10 km	
Star surface imaging	700 m	
Planet mass by microlensing	15 km	
Giant planet radius	6 km	
Giant planet 3×3 px. cartography	18 km	
Biosignatures		2000

6.1 Conclusions

The main conclusion is that the majority of the most significant objectives, which will make a breakthrough in planet characterization, will be satisfied with a 3 - 10 km class interferometer. The total collecting area should be as large as possible in order to access objects possibly fainter than $m = 30$ or a good quality photometry on $m = 25$ objects. If we assign as a final goal the paramount objective of detecting an $m = 30$ Earth in an 1 hour exposure with a SNR = 7 (taking into account only photo noise), the minimum required collecting area is A = 200 m^2. It corresponds for example to 20 3-m telescopes or to 8 5-m telescopes.

The detection of an Earth is not the final goal. Once an Earth will be detected and characterized spectrally, it will become essential to have an idea of the surface morphology of its "vegetal" coverage, necessitating a cartography with at least 20×20 pixels. This ambitious, but inevitable, perspective beyond 2025 will be possible only with baselines of several hundred kilometers, probably in space (Labeyrie 1996).

References

Arnold L., Gillet S., Lardière O., Riaud P., Schneider J., 2002, A&A 392, 231

Arnold L., Schneider J., 2004, A&A 420, 1153

Brown R., Burrows C., Casertano S. et al, 2003, In: Future EUV/UV and Visible Space Astrophysics Missions and Instrumentation", SPIE Publications Vol 4854, p. 95

Clark R.N. 1999, Spectroscopy of Rocks and Minerals, and Principles of Spectroscopy (J. Wiley and Sons, ed. A. Rencz, New-York)

Ford E., Seager S. Turner E., 2001, Nature 412, 885

Ghosh H., DePoy D., Gal-Yam A. et al, 2004, ApJ, 615, 450

Ip W., Kopp A., Hu J., 2004, ApJ. Letters 602, L53

Labeyrie A., 1996, A&A Suppl. 118, 517

Labeyrie A., Schneider J., Boccaletti A., Riaud P., Moutou C., Abe L., Rabou, P., 1999, In: Darwin and Astronomy, ESA SP-451, p. 21

Liu M., Najita J., Tokumaga A., 2003, ApJ 585, 372

Martin E., 2004, In: Eds. A. Chalabaev, Y. Fukui and T. Montmerle, Moriond-YLU 2004, in press (astro-ph/0410678)

Merline W., Weidenschilling S., Durda D. et al. 2002, in Asteroids III, Eds. W. F. Bottke, A. Cellino, P. Paolicchi, & R. P. Binzel (Univ. of Arizona), p. 289

Noll K., 2003, Earth, Moon, and Planets 92, 395

Saar S., Cuntz M., Shkolnik E., 2004, In: Eds. Dupree & Benz, Stars as Suns: Activity, Evolution, PlanetsSchneider J. 1999, In: VLT Opening Symposium, Eds. J. Bergeron & A. Renzini. Springer, p. 499

Schneider J., 2003, In: Towards other Earths: Darwin/TPF and the search for extrasolar terrestrial planets. ESA SP-539 p.

Schneider J., Arnold L., Borkowski V., 2003, in: Barret D., Combes F. (eds)Highlights in Astrophysics. SF2A 2003. p. 205

Selsis F., 2003, In: Extrasolar Planets: Today and Tomorrow. Ed. J.-P. Beaulieu, in press

Shkolnik E., Walker G., Bohlender D., 2003, ApJ 597, 1092

Sromovsky I., Fry P., Limaye S. Baines K., 2003, Icarus 163, 256

Stevens I., 2004, submitted to MNRAS

Sudarsky D., Burrows A., Hubeny I., 2002 ApJ 588, 1121

Tinney C., Tolley A., 1999, MNRAS 304, 119

Witteborn F., Bregman J., Pollack J., 1979, Science 203, 643

Zapatero-Osorio R., Béjar V., Martin E., Rebolo R., Barrado y Navascués D., Mundt R., Eislöffel J., Caballero J., 2002, ApJ 578, 536

Zarka Ph., Treuman R., Ryabov B., Ryabov V. 2001, Ap&SS, 277, 293